

# Non-steady state 2D numerical simulation of gas–liquid phase transition in metal vapour

Jevgenijs Kaupuzs and Janis Rimshans

*Institute of Mathematics and Computer Sciences, University of Latvia,  
LV-1459, Rainja Boulevard 29, Riga, Latvia*

(Received August 26, 1999)

A mathematical model of diffusion of vaporized interacting metal molecules in a fireproof material is considered. The model is based on microscopic kinetic equations describing the process under condition of a strongly non-homogeneous temperature field. A two-dimensional structure is examined, where the inner hot surface acts as the source of metal vapour and the outer surface – as a cooler. Due to interaction between metal molecules, a phase transition (condensation) proceeds near the outer surface. A conservative, monotonous, and absolutely stable difference scheme is developed on the basis of a special exponential substitution for the concentration of molecules. Results of 2D numerical experiments in non-steady state are presented.

## 1. MATHEMATICAL MODEL AND DIFFERENTIAL EQUATIONS

The problem being studied is related to metal vapour penetration in a ceramic material (nozzle). The heated metal is assumed to flow along the left and the right boundaries of a rectangular ceramic sample of dimensions  $x_L$  and  $y_L$ . We choose the coordinate system so that the  $x$  and the  $y$  axes are oriented along the bottom and the left boundary of the sample, respectively. The left boundary line is maintained at a higher temperature, the right boundary line – at a lower temperature. For this reason the left boundary line is referred to as the heater and the right boundary line as the cooler. Due to the heat source near the cooler the distribution of temperature inside the sample is non-homogeneous.

The two dimensional ceramic sample is considered to be a porous medium wherein the metal molecules migrate. At the microscopic scale the kinetic process is assumed to be stochastic and, due to a non-homogeneous temperature field, formation of a new phase is possible. One-dimensional calculations [1] have shown a possible stochastic nature of phase transition. In the present study the problem is generalized to a two-dimensional geometry. We propose the difference scheme for the two-dimensional case and provide numerical simulation of molecular kinetics.

A method developed earlier [3, 4, 6] is adopted to derive diffusion equation from a microscopic model. The particles (metal molecules) are assumed to occupy the sites of a two-dimensional square lattice, the lattice constant being  $b$ . The neighboring particles attract each other and, provided all the sites are occupied, the binding energy per molecule (two bonds) is  $-\varepsilon$ . Migration of the metal molecules is described as a stochastic process the particles being able to jump from one site to another not occupied by any other particle. To describe the physical situation of molecules moving through pores we have assumed the average distance of a single jump  $a$  being much longer than the lattice constant  $b$ . To derive the diffusion equation, we consider stochastic jumping of a particle between sites with coordinates  $(x, y)$  and  $(x + a, y)$ . At the thermodynamic equilibrium, the probabilities of opposite stochastic events are related to each other by the detailed balance condition. In particular, we have

$$\frac{w_+}{w_-} = \exp\left(\frac{E(x, y)}{KT(x, y)} - \frac{E(x + a, y)}{KT(x + a, y)}\right) = \exp\left(\frac{\varepsilon}{K} \frac{C(x + a, y)}{T(x + a, y)} - \frac{\varepsilon}{K} \frac{C(x, y)}{T(x, y)}\right) \quad (1)$$

where  $w_+$  and  $w_-$  are the probabilities per unit time for the considered particle to jump from the site  $(x, y)$  to the site  $(x + a, y)$  and vice versa, respectively;  $E(x, y)$  is the interaction energy between the particle located at the site  $(x, y)$ , and its neighbors;  $T(x, y)$  is the temperature which at the thermodynamic equilibrium is constant; and  $K$  is the Boltzmann constant. In our model, we have assumed that Eq. (1) remains true if the temperature depends on the spatial coordinates  $x$  and  $y$ , which is motivated as follows. Since the distance of a jump is remarkably longer than the interaction distance  $b$  between particles, the probability per time to initiate the jump depends on the local temperature and local binding energy at the place  $(x', y)$  (where  $x'$  is either  $x$  or  $x + a$ ) from which the jump starts, and is equal to  $\nu \cdot \exp(E(x', y)/KT(x', y))$ . The constant  $\nu$  is the frequency factor characterizing the frequency of "attempts" a given particle makes to overcome the potential barrier. In this case the detailed balance means that Eq. (1) is satisfied. According to the above assumption, transition frequencies are

$$w_{\pm} = \Omega_0 \cdot \exp\left(\pm \frac{1}{2} \left[ \frac{E(x, y)}{KT(x, y)} - \frac{E(x + a, y)}{KT(x + a, y)} \right]\right), \quad (2)$$

where

$$\Omega_0 = \nu \cdot \exp\left(\frac{1}{2} \left[ \frac{E(x, y)}{KT(x, y)} + \frac{E(x + a, y)}{KT(x + a, y)} \right]\right) \quad (3)$$

is the characteristic jumping frequency of a particle. For further simplification  $E(x, y)$  has been replaced by its average value  $-2\varepsilon \cdot C(x, y)$ , where  $C(x, y)$  is the concentration of molecules, normalized to be in the range  $[0, 1]$ . Based on this assumption, the particle fluxes  $f_+(x + a/2, y)$  and  $f_-(x + a/2, y)$  in the positive and in the negative direction, i.e., the number of particles per unit time jumping from site  $(x, y)$  to  $(x + a, y)$  and vice versa, can be evaluated easily. A jump in the positive direction (from  $(x, y)$  to  $(x + a, y)$ ) with the frequency  $w_+$  can occur if the site  $(x, y)$  is occupied by a particle whereas the site  $(x + a, y)$  is free. In the mean field approximation the probability of such an arrangement of particles is equal to  $C(x, y) \cdot (1 - C(x + a, y))$ . Similarly, a jump in the opposite (negative) direction can occur if the site  $(x + a, y)$  is occupied and the site  $(x, y)$  is free, which realizes with the probability  $C(x + a, y) \cdot (1 - C(x, y))$ . According to this consideration and Eq. (2), we have

$$f_{\pm}(x + a/2, y) = \Omega_0 C(x + a/2 \mp a/2, y) [1 - C(x + a/2 \pm a/2, y)] \times \exp\left[\frac{\varepsilon}{K} \left( \frac{C(x + a/2 \pm a/2, y)}{T(x + a/2 \pm a/2, y)} - \frac{C(x + a/2 \mp a/2, y)}{T(x + a/2 \mp a/2, y)} \right)\right]. \quad (4)$$

The flow  $J_x(x + a/2, y)$  of the particles in  $x$  direction can be expressed as:

$$J_x(x + a/2, y) = f_+(x + a/2, y) - f_-(x + a/2, y). \quad (5)$$

The flow of the particles in  $y$  direction at the point  $(x, y + a/2)$  can be expressed in the same way by appropriate substitution (i.e.,  $x$  and  $y$  exchange the roles). The final form for flow expressions is obtained by expanding the values of  $C(x, y)$ ,  $C(x + a, y)$ , and  $C(x, y + a)$  in the vicinity of space points  $(x + a/2, y)$  and  $(x, y + a/2)$  assuming that the variation of  $C(x, y)$  is small within a spatial distance  $a$ . Thus, we obtain:

$$J_x(x + a/2, y) = -\Omega_0 a \cdot \text{ch}(\gamma_{x+a, y}) \frac{\partial C}{\partial x} + 2\Omega_0 C(1 - C) \text{sh}(\gamma_{x+a, y}), \quad (6)$$

$$J_y(x, y + a/2) = -\Omega_0 a \cdot \text{ch}(\gamma_{x, y+a}) \frac{\partial C}{\partial y} + 2\Omega_0 C(1 - C) \text{sh}(\gamma_{x, y+a}), \quad (7)$$

where

$$\gamma_{x+a, y} = \frac{\varepsilon}{K} \left( \frac{C(x + a, y)}{T(x + a, y)} - \frac{C(x, y)}{T(x, y)} \right), \quad \gamma_{x, y+a} = \frac{\varepsilon}{K} \left( \frac{C(x, y + a)}{T(x, y + a)} - \frac{C(x, y)}{T(x, y)} \right). \quad (8)$$

Note that  $C(x, y)$  is the probability that site  $(x, y)$  is occupied. Evolution of this probability with time  $t$  is determined by the sum of partial contributions to  $\partial C(x, y)/\partial t$  due to flows  $J_x(x \pm a/2, y)$  and  $J_y(x, y \pm a/2)$ . Thus, we have

$$\frac{\partial C(x, y)}{\partial t} = -J_x(x + a/2, y) + J_x(x - a/2, y) - J_y(x, y + a/2) + J_y(x, y - a/2). \quad (9)$$

The macroscopic diffusion equation (the flow continuity equation) is obtained from (9) in the limit  $a \rightarrow 0$ , where all quantities in Eq. (9) may be considered as continuous analytical functions of coordinates. Neglecting the terms of order  $a^2$ , we obtain

$$\frac{\partial C}{\partial t} = -a \cdot \text{div } \vec{J}, \quad (10)$$

where  $\vec{J}$  is the flow vector with components  $J_x(x, y)$  and  $J_y(x, y)$  defined by Eqs. (6) and (7).

In the proposed model the macroscopic flow is created not only by the concentration gradient, but also by the temperature gradient which plays the role of an external force. It should be noted that in our further interpretation the phase transition (condensation) is caused by the temperature field created by the heat source. In our opinion, other factors, such as the variation of temperature, the heat conductivity, and the characteristic jumping frequency  $\Omega_0$  due to the change of concentration, are less important. Inclusion of all these factors would not cause principal problems in building up the difference scheme. According to the above arguments the steady-state temperature distribution  $T(x, y)$ , calculated from the usual heat conduction equation

$$\frac{\partial T}{\partial t} = D \nabla \cdot (\nabla T) + Q, \quad (11)$$

has been used as the first approximation in the continuity equation (10), where  $D = \lambda/(c\eta)$  is the heat diffusion coefficient and  $Q$  is the heat source. In this case  $\lambda$  is the heat conductivity,  $c$  is the heat capacity, and  $\eta$  is the density of the heat conducting medium. According to our assumptions, we have chosen constant values for  $\lambda$ ,  $D$ , and  $\Omega_0$ .

In our calculations the diffusion coefficient is assumed to be  $D = 0.001 \text{ m}^2/\text{s}$ . The characteristic jumping frequency and distance are chosen  $\Omega_0 = 10^5 \text{ s}^{-1}$  and  $a = 10^{-5} \text{ m}$ . Dimensions  $x_L$  and  $y_L$  of the structure in the  $x$  and  $y$  directions are taken  $x_L = y_L = 0.1 \text{ m}$ . The source of metal vapour and the cooler are located at the boundary lines  $\Omega_S = (x = 0, 0 \leq y \leq y_L)$  and  $\Omega_C = (x = x_L, 0 \leq y \leq y_L)$ , respectively. The temperatures  $T_S$  and  $T_C$  are constant at the corresponding boundary lines  $\Omega_S$  and  $\Omega_C$ . On the boundary lines  $(y = 0, 0 < x < x_L)$  and  $(y = y_L, 0 < x < x_L)$  derivatives of temperature are equal to zero.

Equation (11) is solved in a traditional way by using the central difference scheme.

## 2. DIFFERENCE SCHEME FOR DIFFUSION EQUATION

One of the problems of numerical solution of the non-linear diffusion equation (10) is the development of an effective difference scheme. In the one-dimensional case, a conservative, monotonous, and absolutely stable exponential type difference scheme has been elaborated [1] for solution of the diffusion equation. In this work, the method developed in [1] is extended to the two-dimensional case.

Let us introduce a nonuniform space grid with steps  $h_i$  ( $i = 1, 2, \dots, M_1$ ) and  $r_j$  ( $j = 1, 2, \dots, M_2$ ). The non-linear diffusion equation (10) is discretized using the balance method. Performing algebraic manipulations, the balance equation is written:

$$\frac{C_{i,j}^{l+1} - C_{i,j}^l}{\tau} = -a \cdot \left\{ \frac{(J_x)_{i+1/2,j} - (J_x)_{i-1/2,j}}{h_i^*} + \frac{(J_y)_{i,j+1/2} - (J_y)_{i,j-1/2}}{r_j^*} \right\}, \quad (12)$$

where:  $\tau$  – the time step,  $l$  – the time step index,  $h_i^* = (h_i + h_{i+1})/2$ ,  $r_j^* = (r_j + r_{j+1})/2$ . In this equation the subscripts  $i \pm 1/2$  and  $j \pm 1/2$  correspond to the middle points of the space grid. To obtain  $(J_x)_{i \pm 1/2, j}$  and  $(J_y)_{i, j \pm 1/2}$  expressions, we have used existing approximation technique [5] for 2D elliptic equation. To get  $(J_x)_{i \pm 1/2, j}$ , first we have to replace concentration  $C(x, y)$  by an unknown function  $W(x, y)$ :

$$C(x, y) = W(x, y) \exp(I_o(x_0, x)), \tag{13}$$

where

$$I_o(x_b, x_f) = \frac{2}{a} \int_{x_b}^{x_f} dx (1 - C) \operatorname{th}(\gamma_{x+a, y}),$$

and  $x_0$  is an arbitrary real number which does not affect the coefficients in the final form of the difference scheme. A tractable form for the flow  $J_x$  expression can be obtained if Eq. (6) is substituted by Eq. (13):

$$J_x = -\Omega_0 a \cdot \operatorname{ch}(\gamma_{x+a, y}) \cdot \exp(I_o(x_0, x)) \cdot \frac{\partial W}{\partial x}. \tag{14}$$

To obtain the flow approximation, the flow  $J_x = (J_x)_{i+1/2, j}$  may be considered as constant within the segment  $x \in [x_i, x_{i+1}]$ . In this case Eq. (14) can be rewritten

$$\frac{(J_x)_{i+1/2, j}}{\operatorname{ch}(\gamma_{x+a, y}) \cdot \exp(I_o(x_0, x))} = -\Omega_0 a \cdot \frac{\partial W}{\partial x}, \tag{15}$$

which, after integration in (15) over the segment  $x \in [x_i, x_{i+1}]$ , yields the grid flow expression

$$(J_x)_{i+1/2, j} = -(\Omega_0 a) \cdot \frac{C_{i+1, j} \cdot \exp(-I_o(x_i, x_{i+1})) - C_{i, j}}{I_d(x_i, x_{i+1})},$$

where

$$I_d(x_b, x_f) = \int_{x_b}^{x_f} dx \frac{\exp(-I_o(x_b, x))}{\operatorname{ch}(\gamma_{x+a, y})}. \tag{16}$$

Assuming  $\operatorname{th}(\gamma_{x+a, y}) \cong \gamma_{x+a, y}$  and  $\operatorname{ch}(\gamma_{x+a, y}) = \operatorname{const}$  within  $x \in [x_i, x_{i+1}]$ , the integration in (16) can be performed easily. Thus, for the grid flow  $(J_x)_{i+1/2, j}$  we have:

$$(J_x)_{k+1/2, m} = -\frac{\Omega_0 a}{h_i} \cdot \operatorname{ch} \left[ \frac{\varepsilon}{K} \left( \frac{C_{k+1, m}}{T_{k+1, m}} - \frac{C_{k, m}}{T_{k, m}} \right) \frac{a}{h_{i+1}} \right] \cdot \beta_{k+1/2, m} \times [1 - \exp(-\beta_{k+1/2, m})]^{-1} [\exp(-\beta_{k+1/2, m}) C_{k+1, m} - C_{k, m}], \tag{17}$$

where:

$$\beta_{k+1/2, m} = \frac{2\varepsilon}{K} (1 - C)_{k+1/2, m} \left( \frac{C_{k+1, m}}{T_{k+1, m}} - \frac{C_{k, m}}{T_{k, m}} \right).$$

A substitution similar to (13) is used for  $J_y$  (7) approximation, with the only difference that integration is performed in  $y$  direction and function  $\gamma_{x+a, y}$  is changed to  $\gamma_{x, y+a}$ . The expression for  $(J_y)_{i, j+1/2}$  can be written by use of substitution  $h_i \Rightarrow r_j$  and  $h_{i+1} \Rightarrow r_{j+1}$  in Eq. (17).

After substitution of  $(J_x)_{i \pm 1/2, j}$  and  $(J_y)_{i, j \pm 1/2}$  in the balance equation (12), the following difference scheme is obtained:

$$\frac{C_{i, j}^{l+1} - C_{i, j}^l}{\tau} = \frac{A_{i, j}}{h_i^*} C_{i-1, j}^{l+1} + \frac{E_{i, j}}{h_i^*} C_{i+1, j}^{l+1} + \frac{B_{i, j}}{r_j^*} C_{i, j-1}^{l+1} + \frac{D_{i, j}}{r_j^*} C_{i, j+1}^{l+1} - Q_{i, j} C_{i, j}^{l+1}, \tag{18}$$

$$1 \leq i \leq M_1 - 1, \quad 1 \leq j \leq M_2 - 1,$$

where:

$$Q_{i,j} = \frac{1}{h_i^*} (A_{i+1,j} + E_{i-1,j}) + \frac{1}{r_j^*} (B_{i,j+1} + D_{i,j-1}).$$

The coefficients  $A_{i,j}$ ,  $B_{i,j}$ ,  $E_{i,j}$ ,  $D_{i,j}$  read:

$$P_{i,j} = P_{i-1/2,j}, \tag{19}$$

$$E_{i,j} = \exp(-\beta_{i+1/2,j}^l) P_{i+1/2,j}, \tag{20}$$

$$B_{i,j} = S_{i,j-1/2}, \tag{21}$$

$$D_{i,j} = \exp(-\beta_{i,j+1/2}^l) S_{i,j+1/2}, \tag{22}$$

$$P_{i-1/2,j} = \Omega_0 a^2 \cdot \text{ch} \left[ \frac{\varepsilon}{K} \left( \frac{C_{i,j}^l}{T_{i,j}} - \frac{C_{i-1,j}^l}{T_{i-1,j}} \right) \frac{a}{h_i} \right] \cdot \beta_{i-1/2,j}^l \cdot \left[ h_i \cdot \left( 1 - \exp(-\beta_{i-1/2,j}^l) \right) \right]^{-1},$$

$$S_{i,j-1/2} = \Omega_0 a^2 \cdot \text{ch} \left[ \frac{\varepsilon}{K} \left( \frac{C_{i,j}^l}{T_{i,j}} - \frac{C_{i,j-1}^l}{T_{i,j-1}} \right) \frac{a}{r_j} \right] \cdot \beta_{i,j-1/2}^l \cdot \left[ r_j \cdot \left( 1 - \exp(-\beta_{i,j-1/2}^l) \right) \right]^{-1}.$$

It can be shown that the half-implicit difference scheme (18) is conservative and the coefficients (19)–(22) satisfy the known monotony conditions. Besides, numerical calculations have shown that difference scheme (18) is absolutely stable.

In the calculations presented below, it is supposed that at time  $t = 0$  the value is assigned from segment  $[0, 1]$  for concentration  $C$  on the boundary lines  $\Omega_S$  and  $\Omega_C$ . On the other boundary lines, the normal component of concentration gradient is kept zero. The initial condition is  $C \equiv 0$  inside the structure.

The system of linear equations (18) was solved by the *ILUCGS* method [2].

### 3. RESULTS OF CALCULATIONS

A nonhomogeneous stationary distribution of concentration is expected at large enough interaction energies normalized to  $KT$ . This can be demonstrated by analytic formulae in the case of the thermodynamic equilibrium when  $\nabla T \equiv 0$ . The homogeneous distribution is stable with respect to any small perturbation if the particle flow is opposite to the concentration gradient. In this case any local concentration maximum dissolves since the particles flow out from the maximum region. The opposite process, i.e., growth of a local maximum occurs if the particle flux is oriented in the same direction as the concentration gradient. This leads to instability of the homogeneous distribution and formation of a nonhomogeneous concentration profile. Such a phenomenon has been studied in [3]. In our model, this phenomenon is interpreted as a phase transition or condensation of metal molecules. According to Eqs. (6)–(7) at  $\nabla T \equiv 0$  this occurs if

$$2C \cdot (1 - C) \cdot \frac{\varepsilon}{KT} > 1.$$

The marginal value of  $\varepsilon$  corresponds to zero particle flux at any small concentration gradient. From this inequality we see that the phase transition occurs at certain concentrations which are larger than some lower critical concentration and smaller than some upper critical concentration, if the condition  $\varepsilon > 2KT$  is satisfied. For  $\nabla T \neq 0$  the same qualitative behavior takes place, as it is evident from our calculations. The phase transition is observed at remarkably smaller values of  $\varepsilon/(KT)$  as compared to the case  $\nabla T \equiv 0$ . At the given temperature distribution in our calculations, the phase transition appears for  $\varepsilon > 0.002$  eV which means that for  $\varepsilon \leq 0.002$  eV the concentration distribution always is homogeneous. Besides, the nonhomogeneous distribution is possible for  $\varepsilon > 0.002$  eV only if the concentration on the boundary lines exceeds the critical value  $C^* \approx 0.2$ .

In the first example of simulation the heat source is located closer to the cooler:  $Q = 1000$  K/s in  $\Omega$ ,  $\Omega = (0.4x_L \leq x \leq 0.8x_L, 0.4y_L \leq y \leq 0.6y_L)$ , otherwise  $Q = 0$ . The temperatures of the source and the cooler are kept constant and equal  $T_S = T_C = 300$  K.

The steady state distribution of temperature is shown in Fig. 1. From Fig. 1 we see that a strongly non-homogeneous temperature distribution arises only in the  $\Omega$  region.

Calculations have been performed at  $\varepsilon = 0.012$  eV with concentrations  $C_S$  and  $C_C$  on the boundary lines  $\Omega_S$  and  $\Omega_C$  both smaller and larger than the critical concentration  $C^* \cong 0.2$ . At  $C_S = C_C = 0.1 < C^*$  the steady-state distribution is homogeneous, i.e.,  $C$  takes the value 0.1 which is equal to the given boundary concentration. At  $C_S = C_C > C^*$  the steady-state concentration distribution is nonhomogeneous, as shown in Fig. 2 where  $C_S = C_C = 0.3$ .

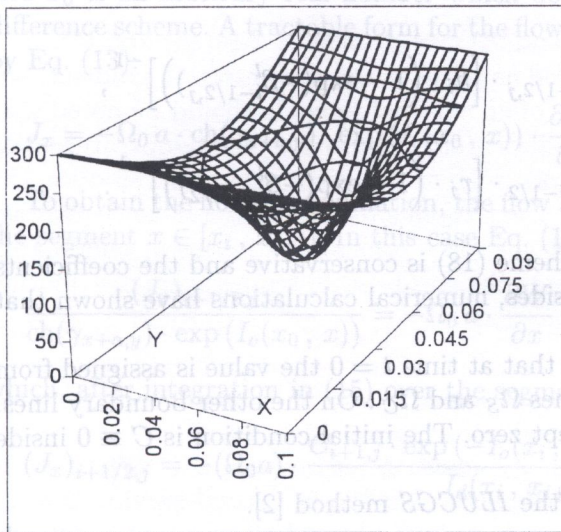


Fig. 1. Steady-state distribution of temperature.

Thermal source is located near the cooler

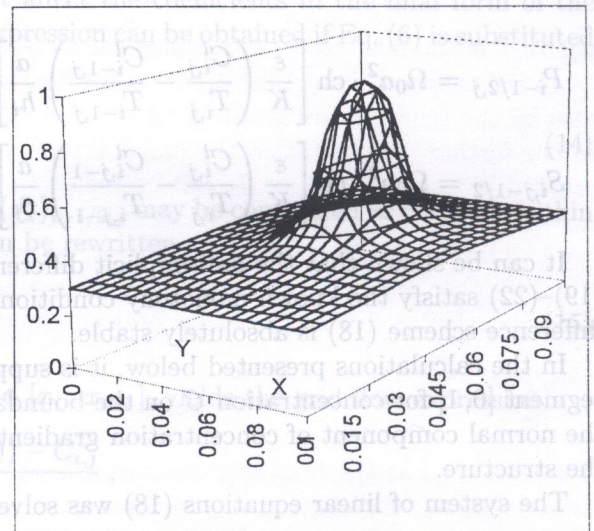


Fig. 2. Steady-state distribution of concentration.

Thermal source is located near the cooler

As it can be seen from numerical calculations, molecules are separated in two regions during the transient kinetic process, and in steady-state, Fig. 2, the gas-liquid type system develops. In such a way, our calculations confirm the qualitative picture outlined at the beginning of this section.

In the second example of simulation it is assumed that  $T_S = 1500$  K and  $T_C = 300$  K, and the heat source is located inside the region beyond the diagonal cross-section:  $Q = 6 \cdot 10^2$  K/s in  $\Omega$ ,  $\Omega = (x \geq y)$ , otherwise  $Q = 0$ . The steady-state temperature distribution is shown in Fig. 3. As shown in Fig. 3, a nonhomogeneous temperature distribution exists over the whole structure, which causes the flow of molecules from the source to the cooler. The considered system is far away from the thermodynamic equilibrium condition.

Concentrations of molecules have been calculated at different values of the bond energy and  $C_S = C_C = 0.3$ , starting with small value  $\varepsilon = 0.002$  eV and going up to values as large as  $\varepsilon = 0.032$  eV. In Fig. 4 the distribution of molecule concentration is shown in the  $y = 0$  cross-section of the structure in the direction from the source to the cooler. As shown in Fig. 4, the concentration of molecules tends to a uniform distribution at small bonding energies, when  $\varepsilon = 0.002$  eV. In this case the distinct nonhomogeneous temperature distribution does not cause a phase transition in the structure. At larger values of the bonding energy ( $\varepsilon = 0.012$  eV and  $\varepsilon = 0.022$  eV), the concentration of molecules is increased near the cooler. A distinct nonhomogeneous distribution of molecules appears at bonding energy  $\varepsilon = 0.032$  eV. In this case, the concentration of molecules reaches values close to the maximum possible  $C = 1$  within a region near the cooler, as shown in Figs. 4 and 5. In Fig. 6 the distributions of molecule concentration in the  $y = 0$  cross-section are

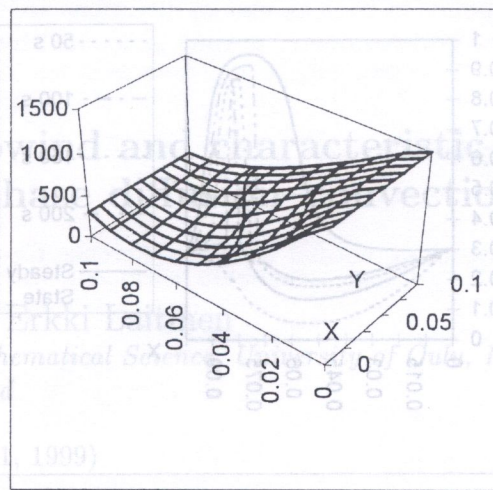


Fig. 3. Steady-state distribution of temperature. Thermal source is located inside the region beyond the diagonal cross-section

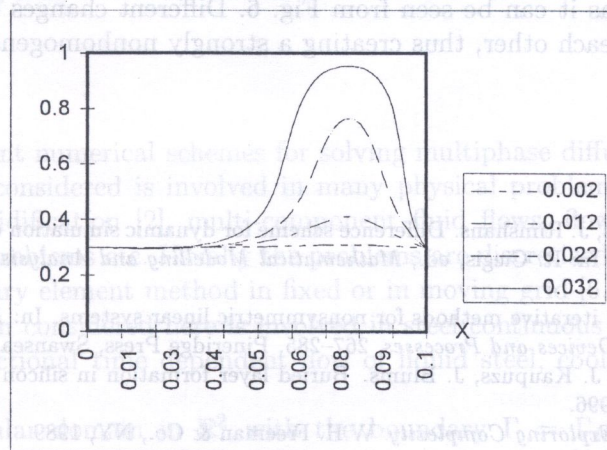


Fig. 4. Distribution of molecule concentration in the  $y = 0$  cross-section

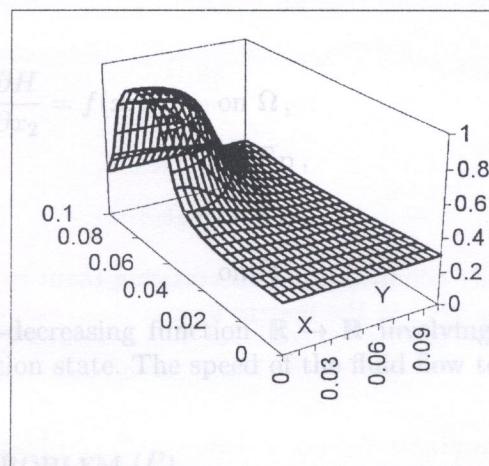


Fig. 5. Steady-state distribution of concentration.  $\epsilon = 0.032$  eV

Comparison of upwind and characteristic schemes for solving multiple diffusion equation

Jali Pieski and

Department of Mathematical Sciences, University of Jyväskylä, PL 3000, 90401 Oulu, Finland

(Received August 31, 1999)

1. INTRODUCTION

In this paper two different numerical schemes for solving multiple diffusion equation are presented. Equation (1) is dependent on the spatial coordinates  $x_1, x_2, x_3$  and time  $t$ . The spatial domain is bounded by  $x_1 \in [0, 1], x_2 \in [0, 1], x_3 \in [0, 1]$  and  $t \in [0, \infty)$ . The initial and boundary conditions are given by (2) and (3). The numerical results are compared with the analytical solution.

The graph of  $H(u)$  is a non-decreasing function of  $u$ . The spatial domain is bounded by  $x_1 \in [0, 1], x_2 \in [0, 1], x_3 \in [0, 1]$  and  $t \in [0, \infty)$ . The initial and boundary conditions are given by (2) and (3). The numerical results are compared with the analytical solution.

$$(P) \begin{cases} \frac{\partial H}{\partial t} - \Delta u + v(t) \frac{\partial H}{\partial x_1} = f(x, t) & \text{in } \Omega, \\ u(x; t) = g_D(x; t) & \text{on } \Gamma_D, \\ \frac{\partial u}{\partial n} = g_N(x; t) & \text{on } \Gamma_N, \\ H(x; 0) = H_0(x) & \text{in } \Omega. \end{cases}$$

The graph of  $H(u)$  is a non-decreasing function of  $u$ . The spatial domain is bounded by  $x_1 \in [0, 1], x_2 \in [0, 1], x_3 \in [0, 1]$  and  $t \in [0, \infty)$ . The initial and boundary conditions are given by (2) and (3). The numerical results are compared with the analytical solution.

2. DISCRETIZATION OF PROBLEM (P)

Let us consider the problem (P) with the boundary  $\Gamma$  divided into two parts:  $\Gamma_D = \{(x_1, x_2) | x_2 = 1/2, x_1 \in [0, 1/2]\}$  and  $\Gamma_N = \Gamma \setminus \Gamma_D$ .

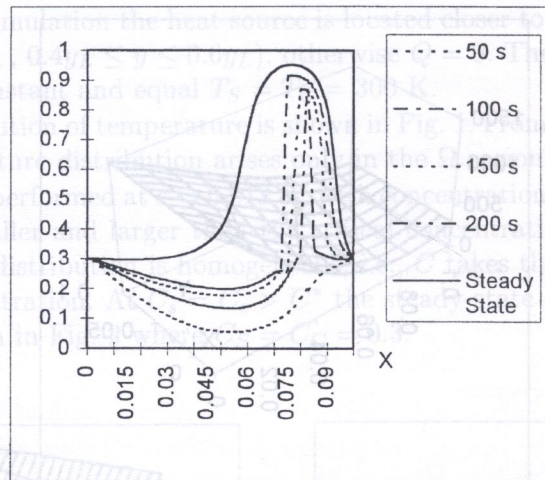


**Fig. 6.** Spatial distribution of molecule concentration in the  $y = 0$  cross-section at various time moments,  $\varepsilon = 0.032$  eV

shown at various time moments (at  $\varepsilon = 0.032$  eV). The spatial distribution of molecules changes nonuniformly with time, as it can be seen from Fig. 6. Different changes can occur at the spatial points which are close to each other, thus creating a strongly nonhomogeneous spatial distribution of concentration.

## REFERENCES

- [1] V. Frishfelds, I. Madzhulis, J. Rimshans. Difference scheme for dynamic simulation describing stochastic kinetics of molecules in ceramics. In: R. Ciegis, ed., *Mathematical Modelling and Analysis*, 93–97, Vilnius, Technika 3, Lithuania, 1998.
- [2] C. Heijer. Preconditioned iterative methods for nonsymmetric linear systems. In: *Proceedings of ITC on Simulation of Semiconductor Devices and Processes*, 267–285, Pineridge Press, Swansea, 1984.
- [3] A. Medvid, I. Madzhulis, J. Kaupuzs, J. Blums. Buried layer formation in silicon by laser radiation. *J. Appl. Physics*, **79**(12): 23–26, 1996.
- [4] G. Nicolis, I. Prigogine. *Exploring Complexity*. W.H. Freeman & Co., NY, 1989
- [5] B.S. Polsky, J.S. Rimshans. Two-dimensional numerical simulation of bipolar semiconductor devices taking into account heavy doping effects and Fermi statistics. *Solid-State Electronics*, **26**(4): 275–279, 1983.
- [6] M. Suzuki, P. Kubo. Dynamics of the icing model near the critical point. *J. Phys. Soc. Japan.*, **24**(1): 50–60, 1968.

In the second example of simulation it is assumed that  $T_s = 1500$  K and  $T_c = 300$  K, and the heat source is located inside the region beyond the diagonal cross section:  $Q = 6 \cdot 10^2$  K/s in  $\Omega$ ,  $\Omega = (x \geq y)$ , otherwise  $Q = 0$ . The steady state temperature distribution is shown in Fig. 3. As shown in Fig. 3, a nonhomogeneous temperature distribution exists over the whole structure, which causes the flow of molecules from the source to the cooler. The flow of molecules is far away from the thermodynamic equilibrium condition.

Concentrations of molecules have been calculated at different values of the bond energy and  $C_s = C_c = 0.3$ , starting with  $\varepsilon = 0.002$  eV going up to values as large as  $\varepsilon = 0.032$  eV. In Fig. 4 the distribution of molecule concentration is shown in the  $y = 0$  cross-section of the structure in the direction from the source to the cooler. As shown in Fig. 4, the concentration of molecules tends to a uniform distribution at small bonding energies, when  $\varepsilon = 0.002$  eV. In this case the distinct nonhomogeneous temperature distribution does not cause a phase transition in the structure. At larger values of the bonding energy ( $\varepsilon = 0.012$  eV and  $\varepsilon = 0.022$  eV), the concentration of molecules is increased near the cooler. A distinct nonhomogeneous distribution of molecules appears at bonding energy  $\varepsilon = 0.032$  eV. In this case, the concentration of molecules reaches values close to the maximum possible ( $C = 1$ ) within a region near the cooler, as shown in Figs. 4 and 5. In Fig. 6 the distributions of molecule concentration in the  $y = 0$  cross-section are